Applications of Steady-State Spray Equations to Combustion Modeling

FREDIANO V. BRACCO*
Guggenheim Laboratories, Princeton University, Princeton, N.J.

A constant cross-sectional area rocket motor was used to study the combustion of a spray of ethanol drops in oxygen. The steady-state spray equation was solved for monodisperse and distributed initial drop radii and for various drag and vaporization rate equations. The local flux of liquid ethanol drops thus calculated was compared with the experimentally determined one for the purpose of selecting a proper over-all spray combustion model. The main conclusion is that a model made up of a Nukiyama-Tanasawa initial drop radii distribution function, a Stokes drop drag equation, and either a modified Priem-Heidmann or a modified Spalding drop vaporization rate equation reproduced accurately the steady state of the engine tested. The original Priem-Heidmann and Spalding vaporization rate equations, which were suggested for single fuel droplets vaporizing and burning in infinite oxidizing media, were found to overestimate the vaporization rate of the droplets within the spray. Moreover, they would have lead to the erroneous conclusion that most of the vaporization occurs in the first few inches of the combustor, and the remaining lingers on at great length, while the actual vaporization is considerably more uniformly distributed in the axial direction. The monodisperse spray models, corresponding to the acceptable distributed spray models, gave acceptable results as well (in this case $r_0 = 5r_{30}/3.915$).

Nomenclature

A = combustion chamber cross-sectional area, cm^2
C_D = drag coefficient
f = drop distribution function, 1/cm^2
K_i = vaporization rate constants, cm^2/sec
K_i^* = modified vaporization rate constants, g/cm sec
Pr = Prandtl number
r = drop radius, cm or μ
r_{30} = volume-number mean drop radius, cm or μ
Re = Reynolds number
t = time, sec
u = velocity, cm/sec
W_F = flux of liquid fuel, g/cm^2 sec
x = distance from the injector, cm
γ = specific heat ratio
μ = viscosity coefficient, g/cm sec
ρ = combustion gas density, g/cm^3
ρ_L = liquid fuel specific gravity, g/cm^3

Subscripts

f = at complete combustion or final values
l = liquid fuel drop
o = at the injector end (at $x = 0$)

Introduction

THE combustion of a spray of fuel droplets in an oxidizing atmosphere is a problem of considerable current interest but far from being quantitatively understood. Our ability to optimize the design of gas turbines, home and industrial furnaces, and direct injection reciprocating and rotary engines (compression ignition or stratified, spark ignition) for minimum emissions and maximum combustion efficiency would be greatly enhanced if reliable mathematical models for the combustion of a spray were available. These models must eventually rely on semiempirical relationships for such spray combustion subprocesses as jet breakup and droplet drag and vaporization. These subprocesses have been actively investigated, both theoretically and experimentally, for over twenty years but only solutions and correlations for oversimplified conditions have so far been obtained.

This study was undertaken to investigate the influence of the various subprocesses on the over-all spray combustion rate and to identify, as well as possible, which semiempirical correlations for the various subprocesses yield the best results when incorporated in an over-all model.

The functional relationships for the jet breakup and for the droplet drag and vaporization, which were found to give theoretical results in agreement with the experimental ones in this study of the ethanol-oxygen system, should be applicable to the previously mentioned, common hydrocarbon-air reactors. However, certain not-too-restrictive conditions must be verified. The chamber pressure must be subcritical, uniform, and steady or varying in space and time so slowly with respect to the moving droplet thermal diffusion time that the quasi-steady vaporization assumption can be adopted. This is the case for the continuous flow reactors and at least for some regions of the operating range of such common intermittent flow reactors as direct injection reciprocating and rotary engines. The spray should be preferably thick. In this study, the interdrop half-distance is estimated to have been of the order of ten drop radii during the most significant fraction of the drop life (say, while 80% of its initial mass vaporizes). Under this condition, which is similar to that existing in most hydrocarbon-air reactors, simple diffusion flames around individual drops are not likely to exist and the vaporization rate is likely to depend more strongly on the gas-drop relative velocity and on the temperature of the gas around the droplet than on the oxidizer mass fraction of this gas (as for the case of a droplet vaporizing without a diffusion flame around it). One obvious consequence of this is a slower vaporization rate for the drop in the thick spray, i.e., a vaporization rate constant which is smaller than the one which would be estimated using data on individual droplets burning in an infinite medium. This, indeed, was found to be the case in this and other studies. Finally, even though these functional relationships may be applicable, the values of some of the constants which appear in them and which gave the best results in this study will remain empirical parameters changing from configuration to configuration. This will

Received January 15, 1974; revision received May 14, 1974. This work, presented at the Combustion Institute Western States Fall Meeting, Monterey, Calif., October 1972, is part of the author's doctoral dissertation. Professor L. Crocco of the Aerospace and Mechanical Science Department of Princeton University was the author's advisor and his help is gratefully acknowledged. This research, under NASA Grant NGL 31-001-115, was sponsored by the Chemical Rocket Division of NASA Lewis Research Center, M. F. Heidmann, Project Manager.

Index categories: Combustion in Heterogeneous Media; Liquid Propellant Rocket Engines.

* Assistant Professor. Associate Member AIAA.

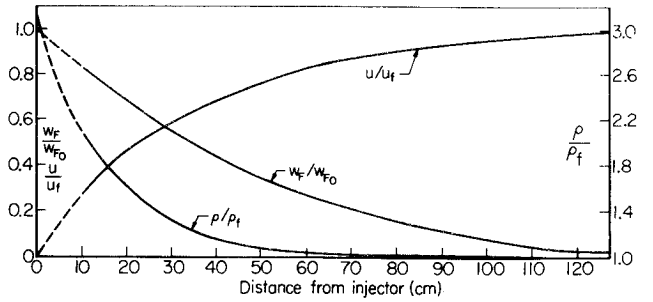

Fig. 1 Experimentally determined liquid fuel flux and gas density and velocity.

be so as long as accurate and detailed solutions of this multidimensional and probably unsteady spray combustion problem are not obtained, i.e., for several years to come.

The study was performed on ethanol sprays burning in gaseous oxygen. A constant (square) cross-sectional area ($6.75 \times 6.75\ cm^2$) rocket motor was used. The chamber pressure was 20 atm, the injection mixture ratio (O/F) was 1.44, and the complete combustion Mach number was 0.158. The injector was made up of 16 impinging like-on-like doublets with a distance between injector units of approximately 1.5 cm. The combustion was steady and took place over a length of over 100 cm. Recirculation was significant only for a small fraction of the total combustion length, within the first 10 cm of the motor (several times the injector unit distance). Past this region, the combustion was uniform on any cross section, i.e., one-dimensional. This situation was confirmed by local temperature and streak photography measurements.

The gas velocity, temperature, density, and composition, as well as the local flux of liquid fuel were determined, vs distance from the injector, by an experimental-analytical method[1,13] which is not discussed in this paper. However, it is important to notice that this method does not require any assumption about the distribution, drag, and vaporization of the fuel drops (accurate and repeatable static pressure measurements by mercury manometers were used instead). This method was extensively applied at three different chamber conditions and its results were cross checked by other independent approaches which included measurements of gas velocity by streak photography,[1] measurements of the characteristic velocity for various chamber lengths,[2] and measurements of velocities and pressures of externally inducted shock waves.[3] The results of interest in this paper are given in Fig. 1. These quantities will be referred to as "experimentally determined." Using the experimentally determined gas velocity and density, the spray equation was then solved for various drag and vaporization models, and the local flux of liquid fuel thus calculated was compared with the experimentally determined one. A model was then considered acceptable if the local flux of liquid fuel calculated by it agreed with the experimentally determined one in trends and magnitude.

Models Studied

The following vaporization rate equations were studied:

$$dr/dt = -K_1/8r \tag{1}$$

$$\frac{dr}{dt} = -\frac{K_2}{8r}[1+0.3Pr^{1/3}Re^{1/2}] \tag{2}$$

$$dr/dt = -(K_3/8r)\,Re^{1/2} \tag{3}$$

$$dr/dt = -(K_4/8r)\,Re \tag{4}$$

$$dr/dt = -K_1{}^*/8\rho r \tag{5}$$

$$\frac{dr}{dt} = -\frac{K_2{}^*}{8\rho r}[1+0.3Pr^{1/3}\,Re^{1/2}] \tag{6}$$

$$dr/dt = -(K_3{}^*/8\rho r)\,Re^{1/2} \tag{7}$$

$$dr/dt = -(K_4{}^*/8\rho r)\,Re \tag{8}$$

where

$$Re = 2r\rho|u-u_l|/\mu$$

$$Pr^{1/3} = [4\gamma/(9\gamma-5)]^{1/3} \approx 0.934$$

The effect of forced convection is absent in the first equation and progressively more important in the following three equations. The fourth equation is herein investigated both to assess the effect of a forced convection dominated vaporization rate equation and because it would simplify steady and unsteady combustion studies. In some of the computations the factor 0.276 instead of 0.3 was used in Eqs. (2) and (6) following Williams[4] (then $0.276\ Pr^{1/3} = 0.258$). The difference between the results obtained with the two factors is small and they are not discussed separately. Most of the study was performed with the drag coefficient either equal to zero (no drag) or with Stokes drag equation ($C_D = 24/Re$). But the case of higher drag was also examined. Droplet breakup was not included. Both the monodisperse and the distributed drop radius cases were studies. In both cases, however, all drops were assumed to have initially the same velocity (u_{l_o}). Theories exist to evaluate the K's appearing in some of the preceding vaporization rate equations as functions of the local chamber conditions.[1,4-6] However, these theories are based on assumptions which are not always verified in a combustion chamber and how the local chamber conditions should be used in those theories also involves some arbitrariness.[1] Furthermore, the K's set the scale for the combustion length. Thus a factor of 2 error in estimating K brings about a similar error in the estimate of the combustion length. For all the abovementioned reasons, the K's were taken to be constant along the combustion chamber and determined by the condition of best agreement between the calculated and the experimentally determined local flux of liquid fuel. Thus the preceding vaporization rate equations have been treated more as probable functional forms than self-consistent applicable vaporization models. Comparison between the K's which gave the best results and those possibly predicted by the corresponding theories were made a posteriori. The initial radius of the drops (r_{30} when distributed initial drop radii were used) has an effect on the computation of the combustion length similar to that of the K's. However, it can more accurately be estimated, at least for the engine configuration presently under consideration, using the results of Ingebo.[7] Accordingly, its value was changed but only within the relatively narrow, predicted limits. A listing of the models which were reviewed is given in Table 1.

Before discussing the individual models in some detail, it might be helpful to point out a characteristic that they exhibited. The models examined could be classified acording to the following criterion. At one extreme there are those models which are controlled by the effect of the relative velocity between gas and liquid drops and the local flux of liquid fuel yielded by them behaves like the dashed line in Fig. 2. Model A8 represents such an extreme: the drag is zero so that $u_l = u_{l_o} = \text{const}$ and the relative velocity is large, the vaporization rate equation is strongly dependent on the relative velocity and the vaporization rate, far from the injection, is further enhanced by the presence of the $1/\rho$ term. At the opposite extreme there are those models which are controlled by the effect of the drop radius and their W_F/W_{F_o}

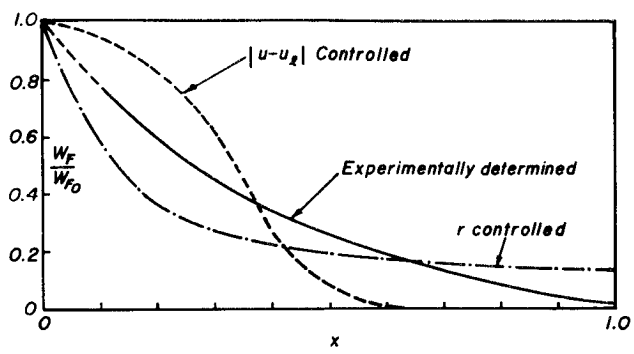

Fig. 2 Trends of calculated vs measured liquid fuel flux.

Table 1 Summary of the models examined and their degrees of acceptability

1) $\frac{dr}{dt} = -\frac{K_1}{8r}$ 5) $\frac{dr}{dt} = -\frac{K_1^*}{8\rho r}$

2) $\frac{dr}{dt} = -\frac{K_2}{8r}[1+0.28\,Re^{1/2}]$ 6) $\frac{dr}{dt} = -\frac{K_2^*}{8\rho r}[1+0.28\,Re^{1/2}]$

3) $\frac{dr}{dt} = -\frac{K_3}{8r}Re^{1/2}$ 7) $\frac{dr}{dt} = -\frac{K_3^*}{8\rho r}Re^{1/2}$

4) $\frac{dr}{dt} = -\frac{K_4}{8r}Re$ 8) $\frac{dr}{dt} = -\frac{K_4^*}{8\rho r}Re$

u_{l_o}	r_o	C_D		1	2	3	4	5	6	7	8
Monodisperse	Monodisperse	0.0	A	N	N	N	N	N	N	N	N
Monodisperse	Monodisperse	$<24/Re$	B	...	Y*	Y*	...	N*	N*	N*	N*
Monodisperse	Monodisperse	$24/Re$	C	N	N	N	N	N	Y	Y	N
Monodisperse	Monodisperse	$>24/Re$	D	N*	N*	N*	N*	...	...	...	...
Monodisperse	Distributed	0.0	E	N	Y	Y	N	...	N	...	...
Monodisperse	Distributed	$<24/Re$	F	...	M*	M*	...	...	...	...	...
Monodisperse	Distributed	$24/Re$	G	M	M	M	M	Y	Y	Y	Y
Monodisperse	Distributed	$>24/Re$	H	...	N	N*	...	...	M	M	...

N ≡ Not acceptable.
Y ≡ Acceptable.
M ≡ Marginally acceptable.
* ≡ Conclusion deduced from the study of the other cases.

behaves as the dotted-dashed line in Fig. 2. Model D1 represents such an extreme: the drag is high so that the relative velocity quickly tends to zero, the vaporization rate is independent of the relative velocity and far from the injector the vaporization rate is not even enhanced by the presence of the $1/\rho$ term. In fact, it will be seen that it takes a relatively fine balance between the two effects for a model to reproduce accurately the trend of the already known W_F/W_{F_o}. It will thus be possible to conclude that vaporization rate Eqs. (6) and (7), with experimentally determined K_2^* and K_3^* (almost one order of magnitude smaller than those possibly predicted by the theory) and a Stokes drag equation, are necessary to reproduce satisfactorily the already known W_F/W_{F_o} in magnitude and trend, and that the use of the distribution function is not necessary, although it does tend to improve the agreement.

Monodisperse Drop Radius Models

Models: A1–A4 of Table 1

All drops have initially the same radius and velocity and vaporize according to vaporization rate Eqs. (1–4). The drag is zero, the K's are constant and they are selected so as to give the best agreement between the calculated and the experimentally determined W_F/W_{F_o}. The initial drop radius[1] is 95 μ corresponding to the radius of that group of drops whose collective volume (mass) is greater than the collective volume of any other group of drops ($r_o = 5r_{30}/3.915$). The r_{30} was selected using Ingebo[7] data ($55\ \mu \leqq r_{30} \leqq 75\ \mu$). The initial drop radius of 75 μ was also used but the trends of the $r_o = 95\ \mu$ case can be obtained again by properly adjusting the values of the K's. It can be shown[1] that for these models

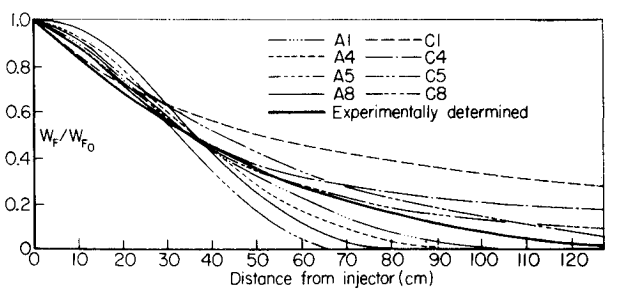

Fig. 3 W_F/W_{F_o} as calculated by Models A1, A4, A5, A8, C1, C4, C5, C8.

$$W_F/W_{F_o} = (r/r_o)^3 \tag{9}$$

and r is determined by the step-by-step integration of the various vaporization rate equations with $u_l = u_{l_o} = \text{const}$. The results of Models A1 and A4 are given in Fig. 3. A2 and A3 gave intermediate trends. Notice that the over-all burning rate is too low near the injector and too high far from it. In these models the effect of the relative velocity is dominant. As long as the relative velocity is low, the combustion rate is also low, but it increases quickly after a proper relative velocity has been reached. Notice also that all the four vaporization rate equations gave essentially the same trend even though their functional forms are quite different. These models were judged unsatisfactory.

Models: C1–C4 of Table 1

Same as previous models except for the drag which now is different from zero. Stokes drag equation is now used: $C_D = 24/Re$. Since the typical Re in these calculations is of the order of 100, Stokes drag is still smaller than that most authors would agree should be experienced by the drops. For these models, Eq. (9) still holds[1] and r is determined by the step-by-step integration of the various vaporization rate equations together with the drag equation

$$\frac{du_l}{dx} = \frac{4.5\mu}{\rho_L r^2}\frac{(u-u_l)}{u_l} \qquad (\text{for } C_D = 24/Re) \tag{10}$$

The results of Models C1 and C4 are given in Fig. 3. C2 and C3 gave intermediate trends. Notice that the over-all burning rate trend is now opposite to that of the previous models. The burning rate is too high near the injector and too low far from it. By adjusting the values of the K's one can obtain good agreement either near the injector (proper local over-all burning rate) or far from it (proper over-all combustion length) but cannot obtain both at the same time. In these models the effect of the drop radius is dominant. The relative velocity tends to become small and the effect of the radius becomes dominant. Notice again that all the four vaporization rate equations gave again similar trends. These models were judged unsatisfactory.

Models: B1–B4 of Table 1

Same as previous models except for $0 < C_D < 24/Re$. No calculations were made for these models but from the study of the previous ones one can conclude that they could conceivably have yielded satisfactory agreement for some proper selection of C_D. This is because the previous two sets of models gave

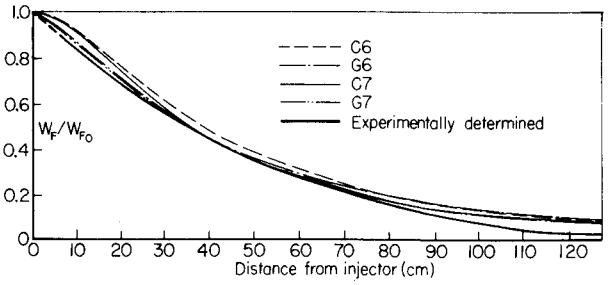

Fig. 4 W_F/W_{F_o} as calculated by Models C6, G6, C7, G7.

opposite over-all burning rate trends and differed only for their C_D. Thus some intermediate C_D function could possibly yield the experimentally determined local fuel flux.

Models: D1–D4 of Table 1

Same as previous models except for $C_D > 24/Re$. No calculations were made for these models but they should worsen the already unacceptable trends of the models for which $C_D = 24/Re$. Increasing the drag, further decreases the relative velocity and the over-all burning rate tends to get even higher near the injector and even lower far from it.

Models: C5–C8 of Table 1

The models in which $C_D = 24/Re$ were judged unsatisfactory because of their high over-all burning rate near the injector. One way of reducing the burning rate near the injector is to make the K's temperature dependent since it is found that the steady-state gas temperature is lower near the injector. It was thus assumed that the vaporization rate is lower where the temperature is lower. The K's were then taken to be proportional to the local gas temperature (but the inverse of the density was actually used in this almost-constant pressure problem) and were replaced by K^*/ρ's where the K^*'s are new constants. This change achieved the goal of reducing the over-all burning rate near the injector and increasing it far from it. Models C6 and C7 (based on the modified versions of the Priem and Heidmann[5] and Spalding[6] vaporization rate equations) were judged satisfactory and the dimensionless liquid fuel fluxes yielded by them are given in Fig. 4. In conclusion, a model using a monodisperse initial drop radius and velocity, a Stokes drag, and a modified Priem and Heidmann or Spalding vaporization rate equation has been found to represent properly the combustion in the engine under configuration. However, the values of the K^*/ρ's are as much as one order of magnitude smaller than those predicted by the corresponding theories.[1] In Fig. 4 the results from the models which include the droplet distribution function are also given although they will be reconsidered later. It can be seen that the distribution function improves the agreement but not in an essential manner.

Models: A5–A8 and B5–B8 of Table 1

It has been seen that in order to get acceptable agreement when a uniform initial drop radius is used, one should either use a $C_D < 24/Re$ and one of the first four vaporization rate equations, or $C_D = 24/Re$ and vaporization rate equations (6) and (7). Both lower drag and lower vaporization rate near the injector serve the purpose of reducing the over-all burning rate near the injector and increasing it far from it. When both effects are combined, the correction is too strong so that Models A5–A8 (see Fig. 3) and B5–B8 are not acceptable.

Models: D5–D8 of Table 1

These models were not explored, but on the basis of the above reasoning they could possibly yield acceptable results.

Distributed Drop Radius Models

In the other models of Table 1, a Nukiyama-Tanasawa initial distribution function for the drop radii was used. The introduction of the distribution function did not change the nature of the results. It just smoothed out the differences making more models acceptable or marginally so. However, a stretching of the combustion length due to the slow burning of the largest drops was noticed. Thus, in general, those models, which with a single initial drop radius tended to give too high an over-all burning rate far from the injector, i.e., the low drag, relative velocity sensitive models, give now better results, the opposite being true for the high drag, radius sensitive, models. Discussion of the individual models involving distributed drop radii follows.

Models: G1–G4 of Table 1

In these models it was assumed that all drops have initially the same velocity but their radii are distributed according to some specified distribution function (soon to be identified as a Tanasawa-Nukiyama type). It was also assumed that there is no nucleation or drop break-up so that drops which initially have the same radius will always have the same velocity [distribution function $f = f(x, r)$]. It can be shown[1] that, under these assumptions, the spray equation[4] reduces to

$$(\partial/\partial x)(u_l f)+(\partial/\partial r)(Rf) = 0 \tag{11}$$

which is equivalent to

$$dr/dx = R/u_l \qquad \text{with} \qquad R \equiv dr/dt \tag{12}$$

$$\frac{d\ln f}{dx} = -\frac{1}{u_l}\left[\frac{\partial R}{\partial r}+\frac{\partial u_l}{\partial x}\right] \tag{13}$$

where the second equation specifies the change of f along lines defined by the first one. In these equations u_l, R, and f are seen as functions of x, r. When Stokes drag is used, Eq. (10) for u_l still applies. Again, the coefficients K_1–K_4 of the vaporization rate equations are constant. Equations (10) and (12) determine $u_l = u_l(x, r_o, u_{l_o})$ and $r = r(x, r_o, u_{l_o})$ when $u = u(x)$ and $\rho = \rho(x)$, given in Fig. 1, are used. While integrating Eqs. (10) and (12), one can also evaluate the changes of f by Eq. (13), but some care must be used since in this equation R and u_l must be seen as functions of x and r. However, u_l is not explicitly known as a function of x and r but it is implicitly defined as such by Eqs. (10) and (12). Thus Eq. (11) was numerically solved[1] for the various vaporization rate equations. A number of observations can be made before answering the question of whether these models are satisfactory or not.

Equation (13) can be written as follows:

$$\frac{f(x,r)}{f_o(0,r_o)} = \exp\left\{-\int_o^x \frac{1}{u_l}\left[\frac{\partial R}{\partial r}+\frac{\partial u_l}{\partial x}\right]dx\right\} \tag{14}$$

It can then be seen that while integrating Eqs. (10) and (12) one can evaluate the ratio f/f_o without having to specify $f_o(0, r_o)$. This means that one can appreciate the influence of the selected vaporization rate equation and of the selected drag equation on the distribution function without specifying the actual drop distribution function at $x = 0$ and valid for any drop distribution function he may later specify at $x = 0$. Thus, in Figs. 5 and 6 the f/f_o's for models G1 and G4 are given. It can be seen that when

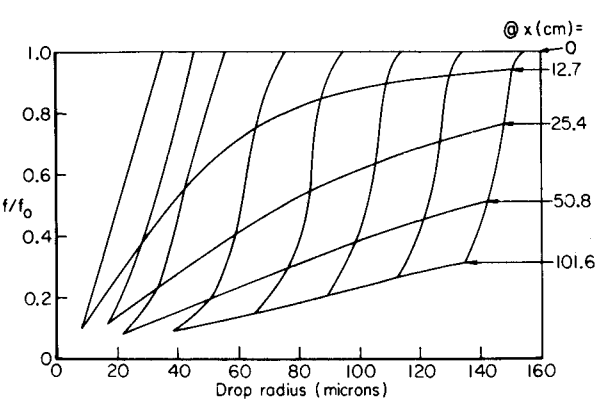

Fig. 5 Distribution function change vs r and x for Model G1.

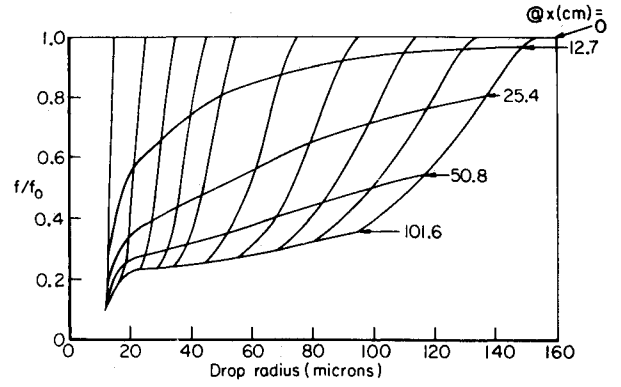

Fig. 6 Distribution function change vs r and x for Model G4.

vaporization rate Eq. (1) is used (Fig. 5), small drops vaporize much faster (inverse dependence on r). Thus, at 12.7 cm from the injector all drops with radius $<35\ \mu$ have practically already been vaporized. On the contrary, large drops vaporize very slowly. Thus at 101.6 cm the radius of the largest drops was reduced only from 155 μ to 134 μ. Or, to put it another way, at 101.6 cm the number of drops having 134 μ radius is still 30% of the original number. Quite a different picture is offered by Fig. 6. Here large drops vaporize much faster and very small drops hardly vaporize at all. Here the vaporization rate equation is independent of the drop radius and depends mostly on the relative velocity; small drops tend to move at the local gas velocity whereas large drops tend to maintain their original velocity. In Fig. 6 one sees that 12 μ drops are still present at 101.6 cm while the largest drop radius at 101.6 cm is only 93 μ. In this case, the horizontal lines indicate that at 101.6 cm the number of drops in all radii groups have been reduced roughly by the same percentage. The number of small drops is reduced mostly near the injector, because of the high initial relative velocity, whereas the number of large drops is reduced mostly far from the injector. In summary, fuel consumption that is high near the injector and low far from it is calculated with vaporization rate Eq. (1). The opposite is true for vaporization rate Eq. (4).

The actual local distribution function $[f = f(x, r)]$ can now be evaluated if the initial distribution function $[f_o = f_o(0, r_o)]$ is specified. Ingebo[7] measured the drop distribution function near the injector in a liquid oxygen-ethanol combustor under firing conditions. He also correlated the volume-mean drop size (r_{30}) to orifice diameter and relative jet gas velocity. An unusual amount of specific information is then available to select the initial distribution function for the engine under consideration. A Nukiyama-Tanasawa distribution function with $r_{o_{max}} = 155\,\mu$ and r_{30} between 50 μ and 70 μ was then selected

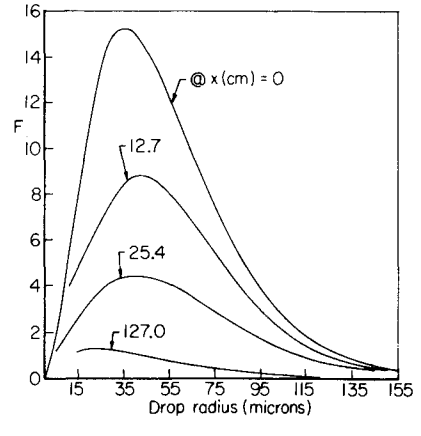

Fig. 7 Distribution function change vs r and x for Model G2, $r_{30} = 70\,\mu$.

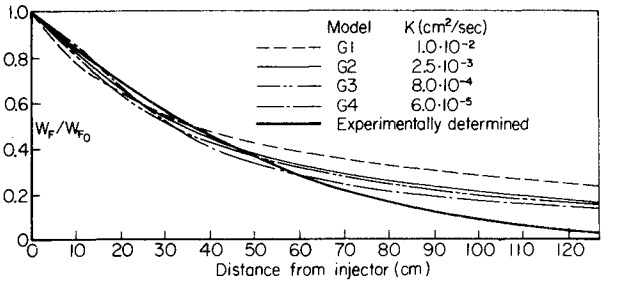

Fig. 8 W_F/W_{F_o} as calculated by Models G1–G4.

$$f_o(0, r_o) = 4Br_o^2 \exp(-3.915\, r_o/r_{30}) \tag{15}$$

and in Fig. 7 an example is given of the calculated local distribution function for the case of Stokes drag, vaporization rate Eq. (2), and $r_{30} = 70\ \mu$. Here the quantity F defined by

$$F = 10^{-1}\frac{f(x, r)}{\int_o^{r_{o_{max}}} f_o\, dr_o} \tag{16}$$

is the local (at x) percentage of the initial (at $x = 0$) number of drops with radius between r and $r + 10\ \mu$.

An interesting question can now be answered. Will the drop radii, initially distributed according to a Nukiyama-Tanasawa distribution function, maintain a similar distribution throughout the engine? In general there is no reason to expect it. If this were the case, one could set

$$f(x, r) = 4B(x)r^2 \exp[-3.915r/r_{30}(x)] \tag{17}$$

and one should get straight lines (of varying slope and intersect) from the following function when evaluated at several x's

$$\ln\left[\frac{f(x, r)}{r^2}\right] = \ln[4B(x)] - \frac{3.915r}{r_{30}(x)} \tag{18}$$

It is thus found[1] that vaporization rate Eqs. (1) and (4) (if very small drops are not included) yield straight lines while vaporization rate Eqs. (2) and (3) do not quite do so.

Having the distribution function $f = f(x, r)$ satisfying the spray Eq. (11), it can be shown[1] that the dimensionless fuel flux can be evaluated by either one of the following two expressions:

$$\frac{d}{dx}\left(\frac{W_F}{W_{F_o}}\right) = \frac{1}{AW_{F_o}}\int_o^{r_{max}(x)} 4\pi r^2 \rho_L R f\, dr \tag{19}$$

$$\frac{W_F}{W_{F_o}} = \frac{1}{AW_{F_o}}\int_o^{r_{max}(x)} \frac{4}{3}\pi r^3 \rho_L u_l f\, dr \tag{20}$$

A check is thus available on the accuracy of the various numerical solutions. The preceding two expressions must yield the same (W_F/W_{F_o}) for all x's. Calculations show that when u_l is constant the above check is met exactly whereas in the more complicated cases in which u_l is a function of both r and x the check is met with decreasing accuracy for increasing x, but the difference is still negligible for the purpose of these computations.

The basic question of whether these models are adequate or not can now be answered with the help of Fig. 8. As this figure shows, all the four vaporization rate equations are satisfactory for the first part of the engine, but tend to give too long a combustion length. Alternatively, by properly selecting the values of K_1–K_4, one could have had good agreement on the combustion length but then the combustion, as calculated by these vaporization rate equations, would have been much too active near the injector. In conclusion, these models are not completely satisfactory. Before going to other models, it might be pointed out that the values of the constants K_1–K_4 and of r_{30} have a strong influence on the over-all solution. This is adequately demonstrated in Fig. 9.

Models: G5–G8 of Table 1

The previous models are not quite acceptable because they give an over-all combustion rate which tends to be too high near

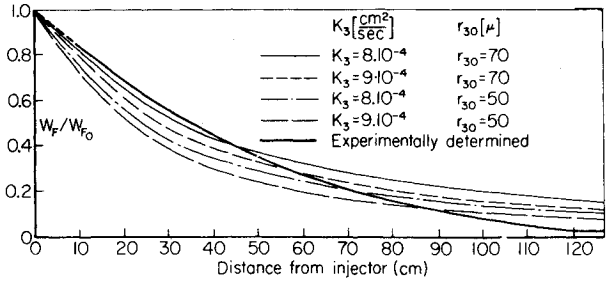

Fig. 9 Influence of K_3 and r_{30} on W_F/W_{F_0}, Model G3.

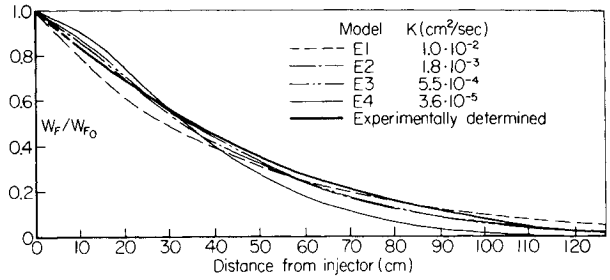

Fig. 11 W_F/W_{F_0} as calculated by Models E1–E4.

the injector and too slow far from it. Thus, if instead of using the K's one used the K^*/ρ's, as in Models C5–C8, one can expect a better agreement since the substitution achieves the goal of reducing the vaporization rate near the injector and of increasing it far from the injector. Accordingly, the vaporization rate equations given by Eqs. (5–8) were used again, together with a Nukiyama-Tanasawa initial drop distribution function and Stokes drag. Figure 10 shows that now all four vaporization rate equations give satisfactory results. Vaporization rate Eqs. (6) and (7) could possibly be selected as those giving better results while vaporization rate Eq. (8) might still be considered acceptable and it is attractive for its mathematical simplicity

$$dr/dt = -(K_4^*/4\mu)|u-u_l| \tag{21}$$

It can be shown that with this vaporization rate equation and with $C_D = 24/Re$ closed-form solutions of the spray equation can be obtained for some specific $u = u(x)$ functions.

Models: E1–E4 of Table 1

In these models, a Nukiyama-Tanasawa initial drop distribution function was again selected and the spray equation was solved but with the somewhat unrealistic assumption of no drag (all drops move at constant speed) and with the vaporization rate Eqs. (1–4). Figure 11 shows that vaporization rate Eqs. (2) and (3) would give again reasonably good results. Indeed in these models one has again decreased the over-all burning rate near the injector and increased it far from it. This was achieved not through a modification of the vaporization rate equations, but through a modification of the drag equation. (Parenthetically, notice that the assumption of constant drop velocity also improved the result obtained with the vaporization rate Eq. (1) in which the relative velocity does not appear at all. This is because the space rate of change of r still depends on u_l [Eq. (12)] and so do the distribution function [Eq. (13)] and the dimensionless fuel flux [Eqs. (19) or (20)]. Also notice that the vaporization rate Eq. (4), which depends heavily on the relative velocity, now gives too high a rate of over-all combustion far from the injector.)

Conclusions

It was concluded that a spray model made up of a Nukiyama-Tanasawa initial drop distribution function, a Stokes drag equation, and either one of the following two vaporization rate equations:

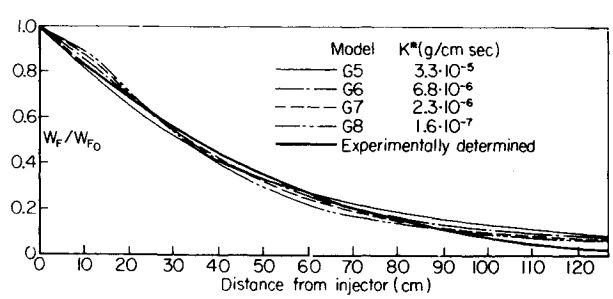

Fig. 10 W_F/W_{F_0} as calculated by Models G5–G8.

$$\frac{dr}{dt} = -\frac{K_2^*}{8\rho r}[1+0.3Pr^{1/3}Re^{1/2}] \quad \text{Modified Priem-Heidmann} \tag{6}$$

$$\frac{dr}{dt} = -\frac{K_3^*}{8\rho r}Re^{1/2} \quad \text{Modified Spalding} \tag{7}$$

reproduced accurately the steady state of the specific oxygen-ethanol engine configuration studied (models G6 and G7). However, it must be noted that the coefficients K_2^*/ρ and K_3^*/ρ represent ad hoc modifications to the vaporization rate equations suggested by Priem-Heidmann and Spalding, respectively. These vaporization rate equations in their original forms reproduced poorly the actual steady state. They led to overestimating the over-all burning rate near the injector and underestimating it far from the injector, or equivalently, they led to the erroneous conclusion that most of the ethanol is burned in the first few inches near the injector and the remaining lingers on at length. The actual combustion is considerably more uniformly distributed in the axial direction. In general, the theoretical vaporization rate constants were found to be too large. To obtain agreement with the experimental data it was found necessary to reduce their values by as much as one order of magnitude.[1] This trend had previously been pointed out by several authors, both for individual drops[11] and for sprays.[12] It was also found that the use of the distribution function is not necessary to reproduce accurately the over-all steady combustion although it does tend to improve the results (i.e., models C6 and C7 are acceptable). The proper initial drop radius to be used when a distribution function is not used is $r_o = 5r_{30}/3.915$. In this study the typical drop Reynolds number was of the order of 100. Nevertheless Stokes drag equation was found to give better results than higher drag equations. In rocket combustion studies much stronger drag equations are often used[8] following Rabin[9] who suggested accounting for the droplet flattening at high Reynolds number. However, Eisenklam et al.[10] noticed no flattening for Reynolds numbers up to 400 and actually suggested lower drag for burning drops than for solid spheres. The findings of this work are in agreement with Eisenklam results, even though the introduction of specific droplet breakup equations could possibly make the higher drag models acceptable.

References

[1] Bracco, F. V., "The Direct Method as Applied to Liquid Rocket Engine Combustion and Explosion Problems," Ph.D. thesis, June 1970, Princeton University, Princeton, N.J.; available as Rept. 71-14359 at the University Microfilms, Xerox Co., 300 N. Zeeb Rd., Ann Arbor, Mich. 48106.

[2] Harrje, D. T., Lee, D. H. et al., "Nonlinear Aspects of Combustion Instability in Liquid Propellant Rocket Motors," Aeronautical Engineering Rept. 553c, June 1963, Princeton University, Princeton, N.J.

[3] Bracco, F. V., Harrje, D. T., and Crocco, L., "Use of Shock Waves to Study Combustion Parameters," CPIA Publication 183, Dec. 1968, Chemical Propulsion Information Agency, Silver Spring, Md., pp. 313–320.

[4] Williams, F. A., *Combustion Theory*, Addison-Wesley, Reading, Mass., 1965.

[5] Priem, R. J. and Heidmann, M. F., "Propellant Vaporization as a Design Criterion for Rocket-Engine Combustion Chambers," TR R-67, 1960, NASA.

[6] Spalding, D. B., "The Combustion of Liquid Fuels," *4th Symposium (International) on Combustion*, The Combustion Institute, Pittsburgh, Pa., pp. 847–864.

[7] Ingebo, R. D., "Photomicrographic Tracking of Ethanol Drops in a Rocket Chamber Burning Ethanol and Liquid Oxygen," TN D-290, 1960, NASA.

[8] Campbell, D. T. and Chadwick, W. D., "Combustion Instability Analysis at High Chamber Pressure," AFRPL-TR-68-179, 1968, Air Force Rocket Propulsion Lab., Wright-Patterson Air Force Base, Ohio.

[9] Rabin, E. A. et al., "The Motion and Shattering of Propellant Droplets," AFOSR TN-60-59, 1960, Air Force Office of Scientific Research, Wright-Patterson Air Force Base, Ohio.

[10] Eisenklam, S. A. et al., "Evaporation Rates and Drag Resistance on Burning Drops," *11th Symposium (International) on Combustion*, The Combustion Institute, Pittsburgh, Pa., 1966, pp. 715–728.

[11] Kumagai, S. and Isoda, H., "Combustion of Fuel Droplets in a Falling Chamber," *The 6th Symposium (International) on Combustion*, The Combustion Institute, Pittsburgh, Pa., 1956, pp. 726–731.

[12] Nuruzzaman, A. S. M., Hedley, A. B., and Beer, J. M., "Combustion of Monosized Droplet Streams in Stationary Self-Supporting Flames," *13th Symposium (International) on Combustion*, The Combustion Institute, Pittsburgh, Pa., 1970, pp. 787–799.

[13] Bracco, F. V., "An Experimental-Analytical Method to Study Steady Spray Combustion," *Journal of Spacecraft and Rockets*, Vol. 10, No. 6, June 1973, pp. 353–354.

NOVEMBER 1974 AIAA JOURNAL VOL. 12, NO. 11

Steady, Incompressible, Swirling Jets and Wakes

ARTUR MAGER*
The Aerospace Corporation, El Segundo, Calif.

The problem of steady, incompressible, swirling, laminar, or turbulent jets and wakes, with their surroundings either in axial motion or at standstill, is formulated in the plane of parameters characteristic of the axial and circumferential velocities. This permits one to discern the physically realistic cases and allows an insight into the behavior of the solutions, particularly near the discontinuities. Examples of continuous (some in closed form) and discontinuous solutions for wakes and jets are given. These show that the axial motion of the surroundings reduces the flow expansion and that the swirling wakes behave quite differently from swirling jets. Good agreement with the available analytical and experimental work of others on swirling jets in still surroundings is indicated.

Introduction

THE method, previously proposed by the author for the study of vortex cores,[1] is extended here to swirling, unbounded flows without net circulation when their surroundings are either in axial motion or at a standstill. These flows are of practical interest because they represent idealizations of real flow situations occurring downstream from propellers, turbojets, air turbines, windmills; and in certain sprays, atomizers and combustion chambers, as well as in models of such natural phenomena as dust devils and water spouts.

In spite of this wide applicability, flows of this kind have received but little attention. Only the swirling jets which issue into still surroundings have been extensively studied analytically and experimentally.[2–10] A review of the analyses reveals that two are quasi-empirical,[4,5] others are restricted to apply when the pressure varies in the axial direction only,[3,9] still others are limited by their experimentally determined constants to certain specific values of the initial swirl[5,10] or by the form and number of the computed expansion terms to conditions away from the origin where the flow is but slightly different from the nonswirling flow.[2] None applies in regions where the swirl is high enough to cause flow reversal. But reversed flows and initial enlargement of the jet's diameter close to the exit nozzle have been observed in such flows by many investigators[5,7,8] and from the practical standpoint of rapid mixing and dispersion they are precisely the features which are most interesting. Therefore, one would like to understand the conditions which lead to such an irregular behavior. This state of knowledge is even more meager when the flow surroundings are in axial motion. To the best knowledge of the author only one experimental investigation of swirling wake has been reported in the literature[11] and the available analytical solutions[11–15] are either limited to weakly swirling far downstream regions[11,12] or apply exclusively to wakes only. For the most part these solutions are continuous and though Gartshore[14] suggested that the discontinuities that he encountered may be the analytical counterpart of the sometimes seen vortex breakdown, he failed to pursue this idea to its full potential. But it is the breakdown of the flow which is perhaps the most interesting feature of swirling wakes because without it, such wakes tend to diffuse very slowly, persisting for long distances behind the generating body—a situation which is often undesirable.

To understand the nature of the solutions, Gartshore[15] plotted their trajectories in a phase plane, that is in the plane of the parameters characteristic of the axial and circumferential velocities, but for some reason he never made the connection between the trajectories and his on-axis condition thus failing to see how the discontinuities arise. Nevertheless, it is this plot of Gartshore's that suggested to the author the method of Ref. 1 which, for flows with circulation, not only afforded a clear insight into the behavior of the solutions close to the discontinuities and at the downstream infinity, but also showed in the case of multiple branch solutions, how crossovers from one branch to another may happen. One would thus expect that the application of this same method to swirling wakes and jets will also permit, in addition to their normal viscous dissipation, the determination of the conditions which lead to their very interesting, irregular behavior.

Phase Plane

Using the quasi-cylindrical approximation, denoting all dimensional quantities by an overbar and dividing all velocities

Presented as Paper 74-35 at the AIAA 12th Aerospace Sciences Meeting, Washington, D.C., January 30–February 1, 1974; submitted February 11, 1974; revision received June 10, 1974.

Index category: Jets, Wakes, and Viscid-Inviscid Flow Interaction.

* Vice President and General Manager, Engineering Science Operations. Fellow AIAA.